Title

"Ligands-with-Benefits": Naphthalene-Substituted Schiff Bases Yielding New Ni(II) Metal Clusters with Ferromagnetic and Emissive Properties and Undergoing Exciting Transformations

Journal

Inorganic Chemistry: including bioinorganic chemistry, 55(3)

ISSN

0020-1669

Authors

Perlepe, Panagiota S

Cunha-Silva, Luís

Gagnon, Kevin J

et al.

Publication Date

2016-02-01

DOI

10.1021/acs.inorgchem.5b02492

Peer reviewed

‘Ligands-with-Benefits’: Naphthalene-substituted Schiff bases yielding new Ni^{II} metal clusters with ferromagnetic and emissive properties, and undergoing exciting transformations

Panagiota S. Perlepe,[†] Luís Cunha-Silva,[‡] Kevin J. Gagnon,[⌂] Simon J. Teat,[⌂] Christos Lampropoulos,[§] Albert Escuer,[#] and Theocharis C. Stamatatos*[,†]

[†] Department of Chemistry, Brock University, St. Catharines, Ontario L2S 3A1, Canada

[‡] REQUIMTE / LAQV & Department of Chemistry and Biochemistry, Faculty of Sciences, University of Porto, 4169-007 Porto, Portugal

[⌂] Advanced Light Source, Lawrence Berkeley National Laboratory, 1 Cyclotron Road, Berkeley, CA 94720, USA

[§] Department of Chemistry, University of North Florida, Jacksonville, FL 32224, USA

[#] Departament de Quimica Inorganica and Institut de Nanociencia i Nanotecnologia (IN2UB), Universitat de Barcelona, Diagonal 645, 08028 Barcelona, Spain

Supporting Information

ABSTRACT: The initial employment of the fluorescent bridging ligand *N*-naphthalidene-2-amino-5-chlorobenzoic acid ($nacbH_2$) in metal cluster chemistry has led to new Ni_{12} (**1**) and Ni_5 (**2**) clusters with wheel-like and molecular-chain topologies, respectively. The double-deprotonated $nacb^{2-}$ ligands were found to adopt four different coordination modes within **1** and **2**. The nature of the ligand has also allowed unexpected organic transformations to occur, as well as ferromagnetic and emission behaviors to emerge. The combined work demonstrates the ability of some ‘ligands-with-benefits’ to yield beautiful structures with exciting topologies and interesting physicochemical properties.

INTRODUCTION

The choice of the organic chelating/bridging ligand is currently one of the most appealing challenges towards the synthesis of new polynuclear 3*d*-metal complexes with diverse physical properties, such as magnetism,[1] optics,[2] conductivity,[3] catalysis,[4] as well as combination of properties (i.e., photomagnetic[5] and multiferroics[6]). The nature, stereo-configuration and electronic properties of the organic chelate are very crucial characteristics and can affect the chemical identities and properties of the resulting polymetallic species.[7] In particular, the type and number of donor atoms (i.e., O and/or N) can facilitate the formation of high-nuclearity metal complexes with moderate-to-high oxidation states (i.e., Mn^{III}, Ni^{II}, etc.), nanoscale dimensions, and beautiful topologies.[8] In addition, the bridging donor atoms of a chelate ligand not only dictate the topology and coordination preferences of the metal ions, but also the nature and strength of the intramolecular magnetic exchange interactions. In an ideal case, ferromagnetic and high-spin molecules may result from the accidental orthogonality of the interacting magnetic orbitals of two or more metal ions *via* the unoccupied orbital(s) of the donor atom.[9]

Apart from the bridging part, the remaining scaffold of an organic chelate is also of importance; aromatic and poly-aromatic chelates are known to (i) enhance the solubility of the metal cluster compounds in solution and subsequently make their crystallization feasible, (ii) provide a rigid, protective ‘shell’ between neighboring molecules in the crystal, (iii) promote energy transfer effects and act as efficient ‘antennas’ towards the enhancement of the complexes’ optical response,[2] and (iv) undergo unusual and unpredicted metal-ion assisted/catalyzed transformations which lead to new organic groups with different properties than the original ones.[4]

For all the above reasons, and more, we have recently started a research program aiming at the exploration of Schiff-base chelates, which are based on the *N*-salicylidene-*o*-aminophenol ($saphH_2$, Scheme 1) scaffold, in Ni^{II} cluster chemistry as a means of obtaining nanosized molecular materials with primarily interesting magnetic properties. Thus, the replacement of the -OH group of the *o*-aminophenol moiety with a carboxylate ($-CO_2H$)

functionality, in conjunction with the addition of a chloro group in place of a phenyl H atom at the 5-position, produced the new ligand *N*-salicylidene-2-amino-5-chlorobenzoic acid ($sacbH_2$, Scheme 1).[10] The latter was proved to be an extremely versatile and capable tetradentate bridging ligand, yielding novel Ni^{II} clusters with record nuclearities (i.e., Ni_{26}[11]) and unprecedented structural topologies (i.e., Ni_{11}[12] and Ni_{18}[11] molecular chains). However, the magnetic properties of $Ni^{II}/sacb^{2-}$ complexes were rather trivial, dominated by antiferromagnetic exchange interactions, and the optical properties of these compounds were negligible, most likely due to quenching effects from the paramagnetic metal ions and/or insufficient energy transfer from the ligand.[11,12]

Based on these findings, and by following a more rational synthetic approach towards the preparation of Ni^{II} clusters with new motifs and additionally interesting magnetic and emission properties, we decided to replace the phenyl ring of the *N*-salicylidene moiety with a naphthalene one. The resulting ligand *N*-naphthalidene-2-amino-5-chlorobenzoic acid ($nacbH_2$, Scheme 1) is still tetradentate as $sacbH_2$, but undoubtedly more rigid and sterically-demanding than $sacbH_2$, thus presaging the isolation of new Ni^{II} clusters. The similarities between the two ligands would also allow for a structural comparison between the $sacb^{2-}$- and $nacb^{2-}$-related coordination compounds. More delighting though with $nacbH_2$ is the presence of the naphthalene substituent, a well-known fluorescent group,[13] which could open new prospects in the field of optics and particularly in the photoluminescence of Ni^{II} metal clusters in the visible region.

Scheme 1. Structural Formulae and Abbreviations of the Ligands Discussed in the Text. The Blue Coloration Illustrates the Different Substituents of the Three Ligands

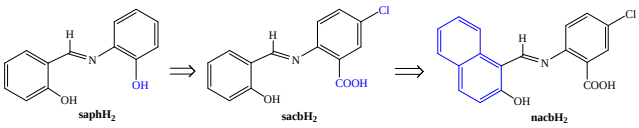

We here report our first results from the initial employment of $nacbH_2$ in Ni^{II} coordination chemistry, which led us to two new Ni_{12} and Ni_5 clusters with interesting molecular topologies, ferromagnetic and emissive behaviours, as well as an exciting $nacbH_2$ to LH_2 ligand transformation, where LH_2 is the 5-chloro-2-[(3-hydroxy-4-oxo-1,4-dihydronaphthalen-1-yl)amino]benzoic acid.

EXPERIMENTAL SECTION

Syntheses. All manipulations were performed under aerobic conditions using chemicals and solvents as received. $nacbH_2$ was prepared in a similar manner as $sacbH_2$.[11,12] Safety note: Perchlorate salts are potentially explosive; such compounds should be synthesized and used in small quantities, and treated with utmost care at all times.

Synthesis of $nacbH_2$. The organic ligand 2-[[(2-hydroxy-1-naphthalenyl)methylene]amino]-5-chlorobenzoic acid or for simplicity *N*-naphthalidene-2-amino-5-chlorobenzoic acid ($nacbH_2$) was prepared in quantitative yields (~93%) by the condensation reaction of 2-amino-5-chlorobenzoic acid (8.58 g, 50 mmol) with 2-hydroxy-1-naphthaldehyde (8.61 g, 50 mmol) in a molar ratio of 1:1 in 100 mL of refluxing MeOH (Scheme S1). The reaction was stirred under reflux for 2 h and then cooled down to room temperature, during which time an orange microcrystalline solid had appeared. The orange solid was collected by filtration, dried under vacuum, and analyzed as solvent-free. Elemental analysis (%) calcd for $nacbH_2$: C 66.37, H 3.66, N 5.08; found: C 66.46, H 3.76, N 4.89. Selected IR data (ATR): ν = 3561 (mb), 3010 (m), 1586 (s), 1543 (s), 1475 (m), 1408 (m), 1361 (s), 1306 (m), 1265 (m), 1231 (w), 1168 (m), 1134 (w), 1111 (m), 1064 (w), 1027 (w), 972 (s), 886 (w), 866 (s), 834 (m), 815 (s), 744 (s), 704 (m), 656 (w), 629 (m), 591 (m), 559 (m), 498 (vs), 437 (m). ^{1}H NMR (DMSO-d^6, ppm): 15.10 (s, 1H, -OH), 13.20 (s, 1H, -COOH), 9.39 (s, 1H, -CH=N), 6.83-8.42 (m, 9H, 9-Ar-H). ^{13}C NMR (DMSO-d^6, ppm): 115.8, 116.9, 118.4, 124.4, 126.3, 127.9, 128.7, 131.4, 132.1, 133.0, 138.2, 138.7, 150.4, 162.9, 193.7.

$(NHEt_3)[Ni_{12}(nacb)_{12}(H_2O)_4](ClO_4)$ (1). To a stirred, orange suspension of $nacbH_2$ (0.07 g, 0.2 mmol) in MeCN (20 mL) was added NEt_3 (56 μL, 0.4 mmol). The resulting yellow solution was stirred for 5 min, during which time solid $Ni(ClO_4)_2{\cdot}6H_2O$ (0.07 g, 0.2 mmol) was added and the color of the solution changed to orange-red. Additional stirring for 20 min did not alter the color or form of the solution. The latter was then filtered, and the filtrate was layered with Et_2O to afford after 5 days yellow blocks of **1**. The crystals were collected by filtration, washed with cold MeCN (2 x 2 mL) and dried under vacuum. The yield was 35 %. Elemental analysis (%) calcd for **1**•$3H_2O$ (M_w = 4916.94 g mol^{-1}): C 54.23, H 3.07, N 3.70; found: C 54.35, H 3.16, N 3.62. Selected IR data (ATR): ν = 2973 (w), 1582 (s), 1553 (vs), 1535 (vs), 1473 (m), 1449 (m), 1427 (s), 1382 (s), 1339 (vs), 1249 (m), 1216 (m), 1179 (m), 1152 (m), 1112 (m), 1089 (w), 1037 (m), 984 (m), 960 (m), 885 (s), 814 (s), 770 (m), 741 (s), 632 (m), 552 (m), 509 (m), 454 (m).

$(NHEt_3)_2[Ni_5(nacb)_4(L)(LH)_2(MeOH)]$ (2): This complex was prepared in the exact same manner as complex **1**, but using MeOH (20 mL) in place of MeCN, under the same aerobic conditions. After 7 days, X-ray quality dark red plate-like crystals of **2** were collected by filtration, washed with cold MeOH (2 x 2 mL) and dried in air. The yield was 50 % based on the total available Ni. Elemental analysis (%) calcd for the solvent-free **2** (M_w = 2807.04 g mol^{-1}): C 58.19, H 3.77, N 4.49; found: C 58.35, H 3.83, N 4.27. Selected IR data (ATR): ν = 2981 (m), 1695 (m), 1574 (vs), 1534 (vs), 1481

(m), 1450 (m), 1404 (s), 1355 (s), 1261 (m), 1217 (m), 1180 (m), 1156 (m), 1111 (mb), 977 (m), 887 (m), 824 (m), 775 (m), 742 (m), 620 (m), 569 (m), 507 (w), 454 (m). The IR band at ~1700 cm^{-1} indicates the presence of quinone-type C=O double-bond in the structure of **2**.

X-ray Crystallography. Data for complex **1** were collected on beamline 11.3.1 at the Advanced Light Source, Lawrence Berkeley National Lab. Samples were mounted on MiTeGen® kapton loops and placed in a 100(2) K nitrogen cold stream provided by an Oxford Cryostream 700 Plus low temperature apparatus on the goniometer head of a Bruker D8 diffractometer equipped with a PHOTON100 CMOS detector operating in shutterless mode. Diffraction data were collected using synchrotron radiation monochromated using silicon(111) to a wavelength of 0.7749(1) Å. An approximate full-sphere of data was collected using a combination of phi and omega scans with scan speeds of 1 second per 4 degrees for the phi scans, and 1 and 3 seconds per degree for the omega scans at 2θ = 0 and -45, respectively. The structures were solved by intrinsic phasing (SHELXT) and refined by full-matrix least squares on F^2 (SHELXL-2014). All non-hydrogen atoms were refined anisotropically. Hydrogen atoms were geometrically calculated and refined as riding atoms. The hydrogen atoms on the water molecules were found in the difference map, their distances fixed, and allowed to refine with a riding model. The triethylammonium and perchlorate ions were severely disordered and have been heavily constrained and modeled as such. Hydrogen positions were calculated on all atoms in these disorder models and included in the molecular formula. There exist a large number of solvent molecules including diethyl ether, acetonitrile, and water. Due to the positional and occupancy disorder of these solvents, stable refinements could not be achieved and as such the density was treated using SQUEEZE[14] as implemented in the software package PLATON.[15,16]

Crystalline material of complex **2** was manually harvested, and a selected single-crystal was mounted on a cryoloop using adequate oil.[17] Diffraction data were collected on a Bruker X8 Kappa APEX II Charge-Coupled Device (CCD) area-detector diffractometer controlled by the APEX2 software package (MoKα graphite-monochromated radiation, λ = 0.71073 Å),[18] and equipped with an Oxford Cryosystems Series 700 cryostream monitored remotely with the software interface Cryopad.[19] Images were processed with the software SAINT+,[20] and the absorption effects were corrected by the multi-scan method implemented in SADABS.[21] The structure was solved using the algorithm implemented in SHELXT-2014,[22,23] and refined by successive full-matrix least-squares cycles on F^2 using the latest SHELXL-v.2014.[22,24] All the non-hydrogen atoms were successfully refined using anisotropic displacement parameters, except from the H atoms of one Et_3NH^+ cation which were only refined with isotropic parameters. Hydrogen atoms bonded to carbon were placed at their idealized positions using appropriate *HFIX* instructions in SHELXL: *43* for the aromatic carbons, *137* for the terminal CH_3, *23* for the CH_2 and *13* for the CH groups. All these atoms were included in subsequent refinement cycles in riding-motion approximation with isotropic thermal displacement parameters (U_{iso}) fixed at 1.2 or 1.5 × U_{eq} of the relative atom. Although the hydrogen atoms of NH-groups in the LH^-/L^{2-} ligands, as well as those of the Et_3NH^+ cation, were neither located from difference Fourier maps nor positioned in calculated positions and refined with isotropic parameters, they were included in the molecular formula of the complex. Substantial electron density was found on the diffraction data, almost certainly due to disordered lattice solvate molecules occupying the spaces created by the packing arrangement of the complexes. Our efforts to locate, model and refine properly these residues were unsuccessful, while the search for the total potential solvent area using the software package PLATON[15,16] confirmed the existence of cavities with potential solvent accessible void volume. Consequently, the original data set was treated with SQUEEZE[14] to minimize the contribution from these highly disordered molecules, and the calculated solvent-free reflection list was then used for the final refinement of the structure. The last difference Fourier map of the crystal structure of **2** revealed the highest peak (4.406 $eÅ^{-3}$) located at 1.29 Å from C11, and it reflects the structural disorder of one of the Et_3NH^+ cations which was not possible to model.

Information concerning crystallographic data collection and structure refinement details is summarized in Table 1. Crystallographic data (excluding structure factors) for the structures of complexes **1** and **2** have been deposited with the Cambridge Crystallographic Data Centre (CCDC) as supplementary publication numbers: CCDC-1426684 (**1**) and 1422591 (**2**). Copies of these data can be obtained free of charge on application to CCDC, 12 Union Road, Cambridge CB2 2EZ, UK; FAX: (+44) 1223 336033, or online via *www.ccdc.cam.ac.uk/data_request/cif* or by emailing *data_request@ccdc.cam.ac.uk*.

Table 1. Crystallographic Data for Complexes 1 and 2

Parameter	**1**	**2**
Formula[a]	$C_{222}H_{144}Cl_{13}N_{13}O_{44}Ni_{12}$	$C_{136}H_{105}Ni_5O_{25}N_9Cl_7$
Fw / g mol^{-1}	4862.86	2806.98
Crystal type	Yellow block	Red plate
Crystal size / mm^3	0.15 □ 0.08 □ 0.06	0.64 □ 0.21 □ 0.03
Crystal	Triclinic	Triclinic

system		
Space group	*P*-1	*P*-1
a / Å	16.9856(6)	18.010(4)
b / Å	25.1456(11)	18.427(4)
c / Å	32.8854(13)	22.874(5)
α / °	72.694(2)	103.960(9)
β / °	84.405(2)	91.535(9)
γ / °	83.388(2)	92.898(10)
V / Å^3	13291.1(9)	7351(3)
Z	2	2
T / K	100(2)	150(2)
D_c / g cm^{-3}	1.215	1.268
μ / mm^{-1}	1.290	0.822
□ range	2.171 – 28.967	3.638 – 25.027
Index ranges	-21 □ *h* □ 21 -31 □ *k* □ 31 -41 □ *l* □ 41	−21 □ *h* □ 21 −21 □ *k* □ 21 −27 □ *l* □ 26
Reflections collected	175095	141055
Independent reflections	54164 (R_{int} = 0.0514)	25733 (R_{int} = 0.0308)
Final *R* indices [I>2□(I)][b,c]	*R*1 = 0.0516 *wR*2 = 0.1186	*R*1 = 0.0528 *wR*2 = 0.1454
Final *R* indices (all data)	*R*1 = 0.0802 *wR*2 = 0.1306	*R*1 = 0.0590 *wR*2 = 0.1506
$(\Delta\rho)_{max,min}$ / e Å^{-3}	2.452 and -1.227	4.406 and -0.773

[a] Excluding lattice solvate molecules. [b] $R1 = \Box(||F_o| - |F_c||)/\Box|F_o|$. [c] $wR2 = [\Box[w(F_o^2 - F_c^2)^2]/ \Box[w(F_o^2)^2]]^{1/2}$, $w = 1/[\sigma^2(F_o^2) + [(ap)^2 + bp]$, where $p = [\max(F_o^2, 0) + 2F_c^2]/3$.

Physical Measurements. Infrared spectra were recorded in the solid state on a Bruker's FT-IR spectrometer (ALPHA's Platinum ATR single reflection) in the 4000-450 cm^{-1} range. NMR spectra were recorded on a Bruker 300 MHz spectrometer at Brock University Chemistry Department. All chemical shifts are referenced to tetramethylsilane ($Si(CH_3)_4$) or residual non-deuterated solvent. Data for proton spectra are reported as follows: chemical shift multiplicity [singlet (s) and multiplet (m)]. Elemental analyses (C, H, and N) were performed on a Perkin-Elmer 2400 Series II Analyzer. Excitation and emission spectra were recorded in the solid-state using a PTI FeliX32 spectrofluorometer. Magnetic susceptibility studies were performed at the University of Barcelona Chemistry Department on a DSM5 Quantum Design magnetometer. Pascal's constants were used to estimate the diamagnetic correction, which was subtracted from the experimental susceptibility to give the molar paramagnetic susceptibility (χ_M).[25]

RESULTS AND DISCUSSION

Synthesis of Ni^{II} Clusters and Organic Ligand Transformations. In order to solely assess the coordination and bridging affinity of $nacbH_2$, we have avoided the use of any additional bridging groups such as carboxylates and/or pseudohalides. Thus, the reaction between $Ni(ClO_4)_2{\cdot}6H_2O$, $nacbH_2$, and NEt_3 in a 1:1:2 molar ratio in MeCN gave yellow crystals of $(NHEt_3)[Ni_{12}(nacb)_{12}(H_2O)_4](ClO_4)$ (**1**) in 35% yield. Although the mechanism of cluster formation is very difficult to be predicted or explained, it is known that the volatility, polarity, rigidity and coordination affinity of reaction solvent(s) are some of the features which affect the identity of the resulting product(s). To that end, the exact same aerobic reaction, but in solvent MeOH instead of MeCN, led to the isolation of dark red crystals of $(NHEt_3)_2[Ni_5(nacb)_4(L)(LH)_2(MeOH)]$ (**2**) in 50% yield.

The new bridging ligand LH_2 (and its anions L^{2-}/LH^-) has been resulted from a complicated and unexpected metal-assisted organic transformation of $nacbH_2$, further highlighting the rich reactivity chemistry of Schiff bases bearing naphthalene groups. Note that this is the first report of LH_2 in both organic and inorganic chemistry. A proposed mechanism of LH_2 formation is shown in Scheme 2, and most likely includes: (i) hydrolysis of $nacbH_2$ to the original precursors, 2-hydroxy-1-naphthaldehyde and 2-amino-5-chlorobenzoic acid,[26] (ii) decarbonylation of 2-hydroxy-1-naphthaldehyde to yield β-naphthol with the subsequent release of HCO_2H,[27] (iii) oxidation of β-naphthol from atmospheric O_2 to the corresponding *o*-naphthoquinone,[28] and (iv) Michael-addition of the NH_2-group of 2-amino-5-chlorobenzoic acid to the β-carbon atom of the naphthoquinone;[29] the resulting LH_2 group could be also in resonance with other quinone/semiquinone-type products in solution. It is noteworthy to mention that the dark red crystals of **2**, opposite to the yellow-green crystals of **1**, are indicative of the formation of a new ligand with a different chromophore than $nacbH_2$; crystalline arylamino-naphthoquinones are known dyes with intense red coloration.[30]

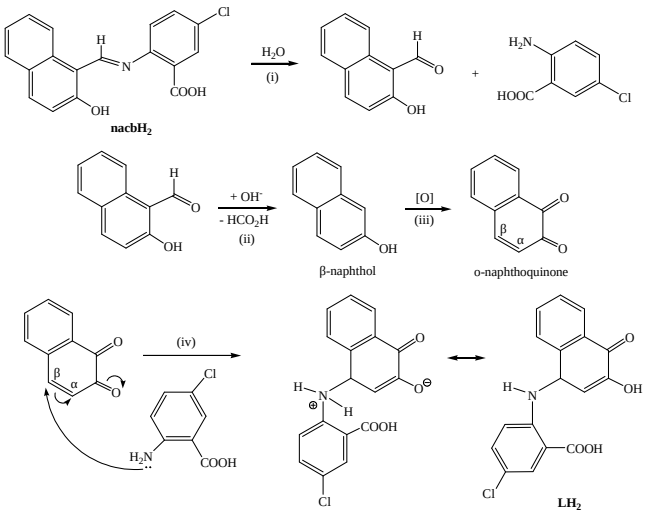

Scheme 2. The proposed simplified mechanism that leads to LH_2, and subsequently to the coordinated, upon deprotonation, LH^- and L^{2-} groups in complex **2**; the Ni^{2+} ions possibly stabilize some of the intermediate products and undoubtedly the final compound **2** (*vide infra*).

Description of Structures. Complex **1** comprises twelve Ni^{II} atoms linked by the carboxylate and naphthoxido O atoms of twelve $nacb^{2-}$ ligands to form a puckered wheel of virtual D_4 point group symmetry (Figures 1 and S1). The void space at the central hole of the wheel is occupied by a $NHEt_3^+$ cation and the overall charge of the Ni_{12} cluster is counterbalanced by a ClO_4^- anion. Four $nacb^{2-}$ groups bind in an $\eta^1{:}\eta^1{:}\eta^2{:}\eta^1{:}\mu_3$ mode (Figure 2), bridging solely through the carboxylate O atoms, in a similar way that $sacb^{2-}$ binds in all the previously reported cluster compounds. The remaining eight $nacb^{2-}$ ligands adopt the $\eta^2{:}\eta^1{:}\eta^2{:}\eta^1{:}\mu_3$ mode (Figure 2), with the two 'pockets' of each ligand chelating a Ni^{II} atom and both the carboxylate and naphthoxido O atoms participating in the bridging of two additional metal ions. This unique coordination mode, responsible for the formation and stabilization of the Ni_{12} wheel, is unprecedented in $Ni^{II}/sacb^{2-}$ chemistry.[10-12]

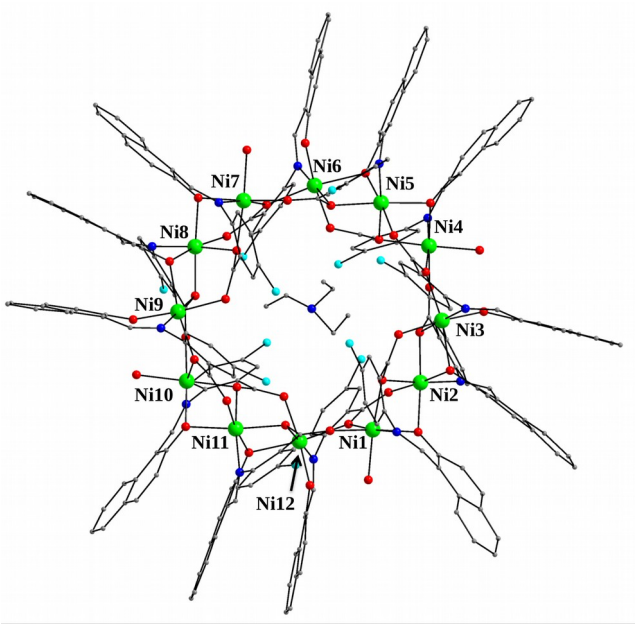

Figure 1. Partially-labelled structure of the cation of **1**. All H atoms are omitted for clarity. Color scheme: Ni^{II} green, O red, N blue, C dark gray, Cl cyan.

We have thus tried to understand the reasons of such coordination differences, which would also allow us to tentatively interpret the structural variations between the $Ni^{II}/nacb^{2-}$ and $Ni^{II}/sacb^{2-}$ products (Figure S2). In all the reported $Ni^{II}/sacb^{2-}$ compounds,[10-12] the ligand's phenyl rings are arranged in an average angle of ~47° from each other. However, the analogous average angle between the naphthalene and phenyl rings of $nacb^{2-}$-related products is ~34°, significantly smaller than that of $sacb^{2-}$. Consequently, the aromatic rings of $sacb^{2-}$ show a higher degree of rotation about the imino 'axle' compared to the naphthalene-benzene pair of $nacb^{2-}$, allowing $sacb^{2-}$ to have a greater flexibility and thus yield a variety of different Ni^{II}_x products. In contrast, the smaller angles between the aromatic rings of $nacb^{2-}$ allow the donor atoms of the ligand to interact differently with the metal ions and consequently stabilize compounds with different topologies than those seen in $Ni^{II}/sacb^{2-}$ products.[10-12]

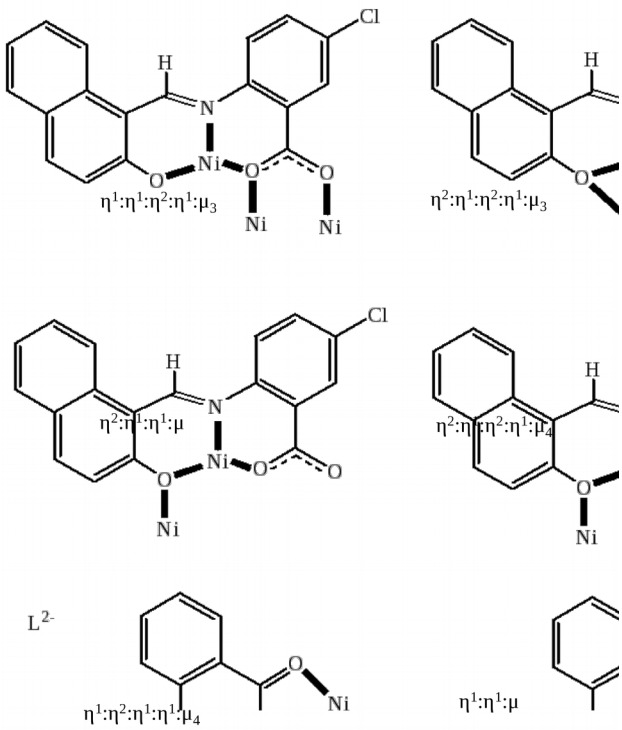

Figure 2. Crystallographically established coordination modes of all organic ligands present in complexes **1** (top) and **2** (middle and bottom).

Hence, the complete core of **1** (including only the doubly-bridging monoatomic groups) is $[Ni_{12}(\mu\text{-}OR)_{20}]^{4+}$ (Figure 3) and can be conveniently described as four bent Ni_3 units (Ni1-Ni2-Ni3, Ni4-Ni5-Ni6, etc., Figure S3) linked at each end by a μ-OR^- group (O8, O17, O26, O35) from a $nacb^{2-}$ ligand. All Ni^{II} atoms are six-coordinate with distorted octahedral geometries. The coordination spheres of Ni(1,4,7,10) are completed by a terminal H_2O molecule; the latter are all strongly H-bonded to the non-bridging phenoxido O-atoms of $nacb^{2-}$. Finally, a space-filling representation (Figure S4) shows the nanoscale dimensions of **1**, with a diameter of ~25 Å and a central hole of ~7 Å diameter; note that the polar surface area of $NHEt_3^+$ is ~3.3 Å^2, justifying its accommodation in the void space of the Ni_{12} wheel. Complex **1** is only the third Ni_{12} wheel-like cluster reported in the literature to date, the two previous ones possessing S = 12[31] and 0[32] spin ground states, respectively.

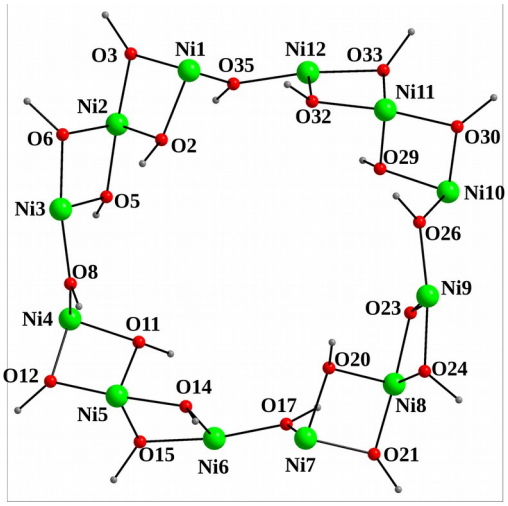

Figure 3. The complete $[Ni_{12}(\mu\text{-}OR)_{20}]^{4+}$ core of **1**. Bond angles (°): Ni1-O2-Ni2 = 92.6(9); Ni1-O3-Ni2 = 94.7(9); Ni1-O35-Ni12 = 116.9(1); Ni2-O5-Ni3 = 95.1(9); Ni2-O6-Ni3 = 97.7(1); Ni3-O8-Ni4 = 116.0(1); Ni4-O11-Ni5 = 92.9(1); Ni4-O12-Ni5 = 95.3(1); Ni5-O14-Ni6 = 96.2(9); Ni5-O15-Ni6 = 96.8(1); Ni6-O17-Ni7 = 116.0(1); Ni7-O20-Ni8 = 91.3(9); Ni7-O21-Ni8 = 95.1(1); Ni8-O23-Ni9 = 95.8(9); Ni8-O24-Ni9 = 96.9 (9); Ni9-O26-Ni10 = 117.3(1); Ni10-O29-Ni11 = 91.4(9); Ni10-O30-Ni11 = 94.4(9); Ni11-O32-Ni12 = 96.1(9); Ni11-O33-Ni12 = 95.7(9).

The crystal structure of **2** consists of $[Ni_5(nacb)_4(L)(LH)_2(MeOH)]^{2-}$ anions (Figure 4) counterbalanced by $NHEt_3^+$ cations; the latter will not be further discussed. The Ni_5 anion comprises a non-linear, zigzag array of five Ni^{II} atoms (av. Ni-Ni-Ni angle = 125.5º) linked together through the naphthoxido (O1, O6, O10, O13), naphthoquinonato (O25), and carboxylate (O2, O3, O8, O9, O16, O17, O18, O19, O22, O23) functionalities of two η^2:η^1:η^1:μ and η^2:η^1:η^2:η^1:μ_4 $nacb^{2-}$ ligands, as well as two η^1:η^1:μ LH^- and an η^1:η^2:η^1:η^1:μ_4 L^{2-} groups (Figure 2). Thus, the overall core of **2**, including the triatomic carboxylate bridges, is $[Ni_5(\mu\text{-}OR)_5(\mu_3\text{-}O_2CR)_2(\mu\text{-}O_2CR)_3]$ (Figure 5), with peripheral ligation provided by the chelating parts of the ligands and a terminal MeOH molecule on Ni1. None of the Ni-O-Ni-O rhombus is planar but instead quite distorted; the average torsion angle is 16.8°. The Ni^{II} atoms are all six-coordinate with distorted octahedral geometries. The differences between the C···O bond lengths (C=O = 1.21-1.23 Å versus C-O = 1.25-1.33 Å) in the coordinated L^{2-}/LH^- ligands are indicative of a hydroquinone-type unit rather than a pure quinone or catechol.[33] Although there are many Ni_5 clusters reported to date, most of them consist of either fused Ni_3 triangular units or strictly linear, Ni-Ni bonded species. Complex **2** is the sixth Ni_5 cluster with a zigzag 'molecular chain' structure reported to date albeit the first non-oximato one.[34]

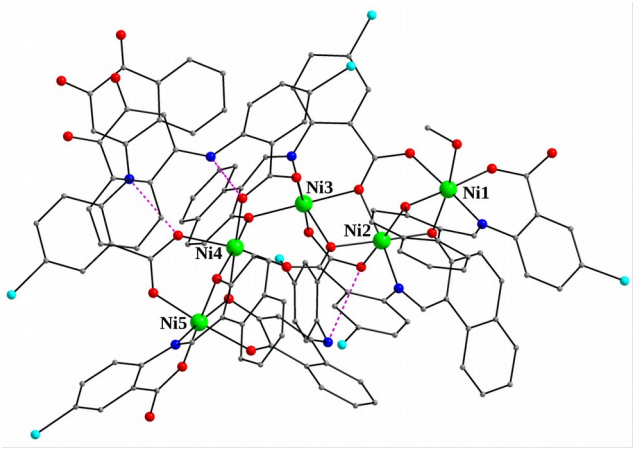

Figure 4. Partially-labelled structure of the $[Ni_5(nacb)_4(L)(LH)_2(MeOH)]^{2-}$ anion of **2**. The purple dashed lines indicate the three strong intramolecular H-bonds between the N-H groups and carboxylate O atoms of the three L^{2-}/LH^- ligands.

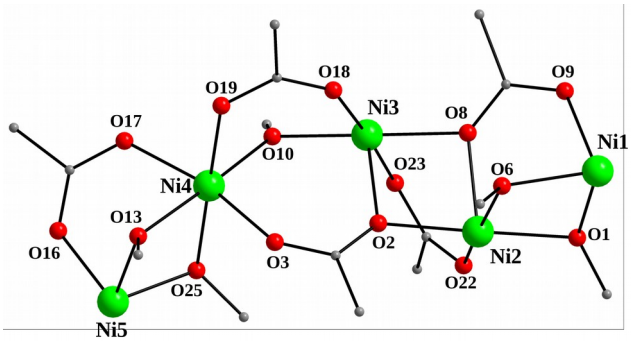

Figure 5. The complete zigzag core of complex **2**. Bond angles (°): Ni1-O1-Ni2 = 95.4(1); Ni1-O6-Ni2 = 94.3(1); Ni2-O8-Ni3 = 97.2(1); Ni2-O2-Ni3 = 98.1(1); Ni3-O10-Ni4 = 110.1(1); Ni4-O13-Ni5 = 92.3(1); Ni4-O25-Ni5 = 94.3(1).

Solid-state Magnetic Susceptibility Studies. Variable-temperature (2.0-300 K range), direct-current (dc) magnetic susceptibility measurements were performed on freshly-prepared microcrystalline solids of **1**·$3H_2O$ and **2**; a dc field of 0.3 T was applied from 30 to 300 K and a weak dc field of 0.03 T was used from 2 to 30 K to avoid saturation effects. The data are shown as $\chi_M T$ versus T plots in Figure 6. For the Ni_{12} wheel, the $\chi_M T$ product steadily decreases with decreasing T, from a value of 13.60 $cm^3mol^{-1}K$ at 300 K to 4.07 $cm^3mol^{-1}K$ at 2 K; such behavior is consistent with the presence of predominant antiferromagnetic exchange interactions between the twelve Ni^{II} atoms. Due to the size, shape, and low-symmetry of **1**, a fit of the experiment data to a theoretical model ($H = -2J_{ij}\hat{S}_i \cdot \hat{S}_j$ convention) turned out to be unsuccessful. Undoubtedly, **1** possesses a small ground state spin value, if not zero. Magnetostructural correlations on complex **1** failed to rationalize, even tentatively, any other than $S = 0$ spin ground state value. An $S = 0$ spin ground state may result from the antiferromagnetic interactions between the four bent Ni_3 units within **1**, promoted by the μ-OR^- groups; the Ni-O-Ni bond angles for the latter monoatomic bridges span the range 116.0-117.3°, clearly suggesting antiferromagnetic interactions between the Ni1···Ni12, Ni9···Ni10, Ni6···Ni7, and Ni3···Ni4 pairs. The two previously reported $[Ni_{12}(chp)_{12}(O_2CMe)_{12}(thf)_6(H_2O)_6]$[31] and $[Ni_{12}(C_{13}H_9N_3O_2)_{12}(MeOH)_{12}]$[32] wheel-like complexes are ferromagnetically- and antiferromagnetically-coupled with $S = 12$ and 0 spin ground states, respectively. This is due to the Ni-O-Ni angles in the former case, which fall into the 95.7-97.4° range, and the large Ni-N-N-Ni torsion angles for the latter case.

In contrast, for the Ni_5 complex (**2**), the $\chi_M T$ product steadily increases from 5.90 $cm^3mol^{-1}K$ at 300 K to a value of 6.65 $cm^3mol^{-1}K$ at 13 K, and then decreases rapidly to a value of 4.64 $cm^3mol^{-1}K$ at 2 K. The data and shape of the plot indicate predominant ferromagnetic exchange interactions between the metal centers. However, the fact that the magnetic susceptibility does not reach the value of ~15 $cm^3mol^{-1}K$, expected for an $S = 5$ system (with $g = \sim 2$), is suggestive of the co-presence of competing antiferromagnetic interactions within **2**. In any case, and for any sign, the magnetic interactions in **2** should be weak.

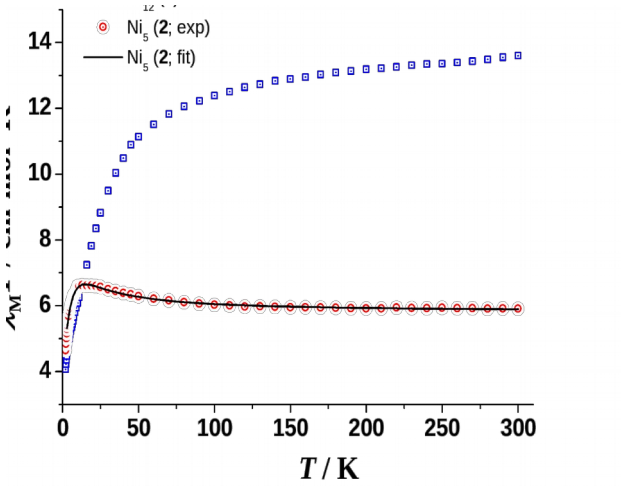

Figure 6. $\chi_M T$ versus T plots of **1**•$3H_2O$ and **2**. The solid line is the fit of the data; see the text for the fit parameters. (inset) J-coupling scheme employed for the elucidation of the magnetic exchange interactions in **2**.

Despite the relatively low-nuclearity of **2**, the fit of the magnetic data was rather challenging due to the low symmetry of the complex and the fact that most of the superexchange pathways consist of countercomplementary carboxylate-alkoxido bridges, with the Ni-O-Ni bond angles close to the F/AF border. The interactions between Ni1···Ni2 and Ni4···Ni5 can be considered very similar (J_1) because they result from the same bridges with

very close bond and torsion angles. However, the remaining superexchange pathways are clearly different from each other (J_2-J_4) and cannot be further simplified to reduce the total number of coupling constants. On the basis of Figure 6 (inset), the applied Heisenberg spin-Hamiltonian for **2** is:

$$H = -J_1(\hat{S}_1\cdot\hat{S}_2 + \hat{S}_4\cdot\hat{S}_5) - J_2(\hat{S}_2\cdot\hat{S}_3) - J_3(\hat{S}_3\cdot\hat{S}_4) - J_4(\hat{S}_1\cdot\hat{S}_3 + \hat{S}_2\cdot\hat{S}_4)$$

The PHI program[35] was used to fit the susceptibility and magnetization data of **2**. An excellent fit (solid line in Figure 6) was obtained with parameters: J_1 = +7.6 cm^{-1}, J_2 = -8.4 cm^{-1}, J_3 = +2.1 cm^{-1}, J_4 = +2.4 cm^{-1} and g = 2.15. To evaluate the reliability of the obtained J_{ij} parameters, we performed a systematic set of fits including a D term or assuming a simpler, linear magnetic structure, excluding the J_4 parameter that accounts for the interaction mediated by the *syn-anti* carboxylate moiety of $nacb^{2-}$ and is much smaller than J_2. In all cases, the sign and magnitude of the remaining J_1-J_3 interactions were practically unaltered. Obviously, the absolute values of the coupling constants are poorly reliable but they agree with the expected values that can be envisaged from the structural data. In particular, the smaller Ni-O-Ni bond angles (related to J_1) promote weak ferromagnetic interactions, whereas the larger Ni-O-Ni bond angles (110.1°, related to J_2) propagate weak antiferromagnetic interactions; finally, the intermediate Ni-O-Ni bond angles and the *syn-anti* carboxylate bridges (corresponding to J_3 and J_4, respectively) promote very weak interactions. As a result of the above reported J values, the ground state cannot be strictly defined, with four consecutive spin states, S = 3, 2, 1 and 4, in a short range of less than 3 cm^{-1}, further justifying the shape and value of magnetization, as shown in Figure 7.

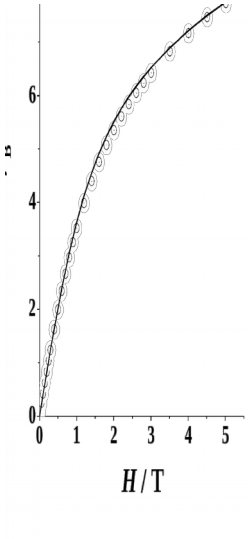

Figure 7. Plot of magnetization (M) versus field (H) for complex **2** at 2 K. The solid line is the fit of the data obtained by using the J coupling constants discussed in the text.

Four different Ni_5 compounds with a zigzag topology have been structurally and magnetically characterized to date. The ferromagnetically-coupled complex $[Ni_5\{pyCOpyC(O)(OMe)py\}_2(O_2CMe)_4(N_3)_4(MeOH)_2]$ has an S = 5 spin ground state in line with the presence of end-on bridging azides and alkoxido groups with Ni-O-Ni angles close to 95°.[34a] For the $[Ni_5(Hpyaox)_4(pyaox)_2L_2](ClO_4)_2$ complex,[34b] where H_2pyaox is the pyridine-2-amidoxime ligand and L is 2-(2-aminoethylamino)ethanol, the overall weak ferromagnetic behavior is due to the particular Ni–N–O–Ni torsion angles which result in different signs and magnitudes of the Ni···Ni magnetic exchange interactions. Complex $[Ni_5(3\text{-Cl-BzO})_4(6\text{-mepao})_4(6\text{-mepaoH})_2(N_3)_2]$, where 6-mepaoH is 6-methylpyridine-2-carbaldehydeoxime ligand and 3-Cl-BzO^- is the 3-chlorobenzoate anion,[34c] has an S = 3 ground state that arises from the combination of antiferromagnetic and ferromagnetic exchange interactions via the triple carboxylate/oximate/oxo bridge, the single oximate bridge and finally the interaction involving the end-on azido bridges. Finally, complex $[Ni_5(RCO_2)_2(dapdo)_2(dapdoH)_2(N(CN)_2)_2(MeOH)_2]$ (R = various) comprises three paramagnetic Ni^{II} centers and two square planar and diamagnetic Ni^{II} atoms bridged together by the anionic forms of the organic chelate 2,6-diacetylpyridine dioxime ($dapdoH_2$).[34e] The compound is antiferromagnetically coupled due to the large Ni-O-N-Ni torsion angles.

Solid-State Emission Studies. The use of metal complexes in the design of luminescent-responsive probes has attracted the interest over the last years, since they can offer improved photophysical responses over the pure organic fluorophores.[2] Thus, in order to gain any possible access into additional physical properties for **1** and **2**, and to compare the optical potency of $nacbH_2$ versus $sacbH_2$, we decided to perform solid-state photoluminescence studies on all compounds at room temperature. The free ligand $nacbH_2$ is a promising 'antenna' group with a pronounced ability for promoting energy transfer effects. Upon maximum excitation at 349 nm, $nacbH_2$ exhibits a strong emission in the 380-420 nm visible range with two clear maxima at 391 and 410 nm, and a weak shoulder at 482 nm (Figure 8). The two maxima are probably due to the presence of two different aromatic groups (naphthalene and benzene) within the same molecule;[36] the emission at ~390 nm is characteristic of the naphthalene functional group.[13] The optical response of $nacbH_2$ in various solutions and different concentrations is exactly the same with that reported in the solid-state. The free ligand $sacbH_2$ has shown a similar emission, albeit with only one emission band at 415 nm, further supporting the fact that the phenyl

emission on this class of Schiff base ligands appears at ~410 nm.[11]

Although there has been no emission detected for any Ni^{II}/$sacb^{2-}$ complex reported to date,[11,12] most likely due to inefficient energy transfer from the ligand and/or quenching effects,[37] this turned out not to be the case for complex **2**. In contrast to the high-nuclearity Ni_{12}, which shows no emission at room temperature, complex **2** exhibits a strong blue-centered emission at 435 nm, upon maximum excitation at 352 nm (Figure 8). The emission of **2** is slightly red-shifted with respect to the free ligand $nacbH_2$ and more intense; the observed and enhanced intensity can be tentatively assigned to the coordination of $nacb^{2-}$ and L^{2-}/LH^{-} ligands to the metal centers. There are no convincing evidences that complexes **1** and **2** retain their structures in solution, and therefore we have not pursued any emission studies in solution.

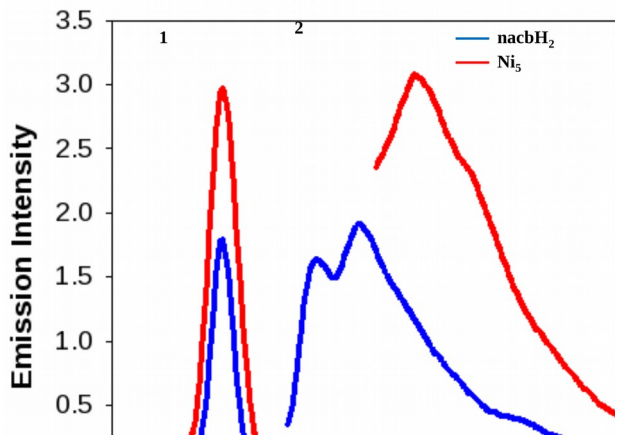

Figure 8. Excitation (1) and emission (2) spectra of $nacbH_2$ (blue lines) and complex **2** (red lines) in the solid-state and at room temperature.

It is known that the deprotonation and coordination of a ligand to a metal ion increases the rigidity of the organic molecule and consequently reduces the loss of energy via vibrational motions.[38] Red-shift of the emission maximum can be normally observed for the most fluorescent compounds in the solid state probably due to the π-π stacking interactions of the aromatic rings in the molecules.[39] Given the complexity of **2**, the number of metal ions and ligands present, among other structural perturbations, a detailed analysis of the photophysical energy transfer mechanism and the type of emission are not feasible. Undoubtedly though, the structural characteristics of $nacbH_2$, and particularly the presence of the naphthalene substituent, have turned this group into a more liable to optical activity ligand than $sacbH_2$.

CONCLUSIONS

In conclusion, we have herein reported a new naphthalene-substituted Schiff base ligand which does not only lead to Ni^{II} clusters with unprecedented topologies and beautiful structures but also contributes to the observation of interesting physicochemical properties, such as ferromagnetic coupling and optical emission, as well as unforeseen organic transformations assisted by the presence of 3*d*-metal ions. Attempts to rationalize the structural and physicochemical differences between the metal clusters obtained with the related $sacbH_2$ ligand were tried out, and these were ascribed to the special steric and electronic properties of $nacbH_2$. Finally, these first findings highlight the importance of selecting an appropriate chelating/bridging 'ligand with benefits' for the synthesis of new molecule-based materials with multiple properties.

ASSOCIATED CONTENT

Supporting Information

Crystallographic data (CIF format), and various structural and magnetism figures. This material is available free of charge via the Internet at http://pubs.acs.org.

AUTHOR INFORMATION

Corresponding Author

* E-mail: tstamatatos@brocku.ca

ACKNOWLEDGMENTS

This work was supported by Brock University, NSERC-DG and ERA (to Th.C.S), the Alexander S. Onassis Public Benefit Foundation (graduate scholarship to P.S.P), the Fundação para a Ciência e a Tecnologia (FCT, Portugal) for financial support to REQUIMTE / LAQV (UID/QUI/50006/2013), and the CICYT (project CTQ2012-30662, to A.E). The Advance Light Source is supported by The Director, Office of Science, Office of Basic Energy Sciences of the U.S. Department of Energy under contract no. DE-AC02-05CH11231. We would also like to thank Professor Dionyssios Papaioannou (Chemistry Department, University of Patras, Greece) for assistance with the proposed mechanism for the formation of L^{2-}/LH^{-} groups in complex **2**. C.L acknowledges support through the Cottrell College Science Award

from the Research Corporation for Science Advancement and the Dreyfus Foundation.

REFERENCES

[1] a) Brechin, E. K. *Chem. Commun*. **2005**, 5141-5143. b) Aromí, G.; Brechin, E. K. *Struct. Bond.* **2006**, *122*, 1-67. c) Tasiopoulos, A. J.; Perlepes, S. P. *Dalton Trans.* **2008**, 5537-5555. d) Stamatatos, Th. C.; Efthymiou, C. G.; Stoumpos, C. C.; Perlepes, S. P. *Eur. J. Inorg. Chem.* **2009**, 3361-3391. e) Milios, C. J.; Winpenny, R. E. P. *Struct. Bond.* **2015**, *164*, 1-109.
[2] Bünzli, J.- C. G.; Eliseeva, S. V. *Chem. Sci.* **2013**, 1939-1949.
[3] a) Jo, M. H.; Grose, J. E.; Baheti, K.; Deshmukh, M. M.; Sokol, J. J.; Rumberger, E. M.; Hendrickson, D. N.; Long, J. R.; Park, H.; Ralph, D. C. *Nano Lett.* **2006**, *6*, 2014-2020. b) Coronado, E.; Martí-Gastaldo, C.; Tatay, S. *Appl. Surf. Sci.* **2007**, *254*, 225-235.
[4] For representative examples see: a) Schmidt, S.; Prodius, D.; Mereacre, V.; Kostakis, G. E.; Powell, A. K. *Chem. Commun.* **2013**, *49*, 1696-1698. b) Brunet, G.; Habib, F.; Cook, C.; Pathmalingam, T.; Loiseau, F.; Korobkov, I.; Burchell, T. J.; Beauchemin, A. M.; Murugesu, M. *Chem. Commun.* **2012**, *48*, 1287-1289. c) Blackman, A. *Eur. J. Inorg. Chem.* **2008**, 2633-2647. d) Chesman, A. S. R.; Turner, D. R.; Moubaraki, B.; Murray, K. S.; Deacon, G. B.; Batten, S. R. *Eur. J. Inorg. Chem.* **2010**, 59-73.
[5] For example, see: Ababei, R.; Pichon, C.; Roubeau, O.; Li, Y.- G.; Bréfuel, N.; Buisson, L.; Guionneau, P.; Mathonière, C.; Clérac, R. *J. Am. Chem. Soc.* **2013**, *135*, 14840-14853.
[6] Long, J.; Rouquette, J.; Thibaud, J. M.; Ferreira, R. A. S.; Carlos, L. D.; Donnadieu, B.; Vieru, V.; Chibotaru, L. F.; Konczewicz, L.; Haines, J.; Guari, Y.; Larionova, J. *Angew. Chem. Int. Ed.* **2015**, *54*, 2236-2240.
[7] a) Winpenny, R. E. P. *Adv. Inorg. Chem.* **2001**, *52*, 1-111. b) Winpenny, R. E. P. *J. Chem. Soc., Dalton Trans.* **2002**, 1-10.
[8] For representative examples, see: a) Tasiopoulos, A. J.; Vinslava, A.; Wernsdorfer, W.; Abboud, K. A.; Christou, G. *Angew. Chem. Int. Ed.* **2004**, *43*, 2117-2121. b) Whitehead, G. F. S.; Moro, F.; Timco, G. A.; Wernsdorfer, W.; Teat, S. J.; Winpenny, R. E. P. *Angew. Chem. Int. Ed.* **2013**, *125*, 10116-10119. c) Scott, R. T. W.; Parsons, S.; Murugesu, M.; Wernsdorfer, W.; Christou, G.; Brechin, E. K. *Angew. Chem. Int. Ed.* **2005**, *44*, 6540-6543. d) Manoli, M.; Inglis, R.; Manos, M. J.; Nastopoulos, V.; Wernsdorfer, W.; Brechin, E. K.; Tasiopoulos, A. J. *Angew. Chem. Int. Ed.* **2011**, *50*, 4441-4444.
[9] a) Kahn, O. *Molecular Magnetism*; VCH Publishers: New York, **1993**; b) Benelli, C.; Gatteschi, D. *Chem. Rev.* **2002**, *102*, 2369-2388.
[10] Perlepe, P. S.; Athanasopoulou, A. A.; Alexopoulou, K. I.; Raptopoulou, C. P.; Psycharis, V.; Escuer, A.; Perlepes, S. P.; Stamatatos, Th. C. *Dalton. Trans.* **2014**, *43*, 16605-16609.
[11] Athanasopoulou, A. A.; Raptopoulou, C. P.; Escuer, A.; Stamatatos, Th. C. *RSC Adv.* **2014**, *4*, 12680-12684.
[12] Athanasopoulou, A. A.; Pilkington, M.; Raptopoulou, C. P.; Escuer, A.; Stamatatos, Th. C. *Chem. Commun.* **2014**, *50*, 14942-14945.
[13] Alexandropoulos, D. I.; Mowson, A. M.; Pilkington, M.; Bekiari, V.; Christou, G.; Stamatatos, Th. C. *Dalton Trans.* **2014**, *43*, 1965-1969.
[14] Van der Sluis, P.; Spek, A. L. *Acta Cryst. A* **1990**, *46*, 194.
[15] Spek, A. L. *Acta Cryst. A* **1990**, *46*, C34.
[16] Spek, A. L. *J. Appl. Crystallogr.* **2003**, *36*, 7.
[17] Kottke, T.; Stalke, D. *J. App. Cryst.* **1993**, *26*, 615.
[18] APEX2, *Data Collection Software Version 2012.4, Bruker AXS, Delft, The Netherlands*, **2012**.
[19] Cryopad, *Remote monitoring and control, Version 1.451, Oxford Cryosystems, Oxford, United Kingdom*, **2006**.
[20] SAINT+, *Data Integration Engine v. 8.27b©*, 1997-2012, Bruker AXS, Madison, Wisconsin, USA.
[21] Sheldrick, G. M. *SADABS 2012/1, Bruker AXS Area Detector Scaling and Absorption Correction Program*, **2012**, Bruker AXS, Madison, Wisconsin, USA.
[22] Sheldrick, G. M. *Acta Cryst. A* **2008**, *64*, 112.
[23] Sheldrick, G. M. *SHELXT v. 2014/3, Program for Crystal Structure Solution, University of Göttingen*, **2014**.
[24] Sheldrick, G. M. *SHELXL v. 2014, Program for Crystal Structure Refinement, University of Göttingen*, **2014**.
[25] Bain, G. A.; Berry, J. F. *J. Chem. Educ.* **2008**, *85*, 532-536.
[26] Cordes, E. H.; Jencks, W. P. *J. Am. Chem. Soc.* **1963**, *85*, 2843-2848.
[27] Ukhin, L. Y.; Morkovnik, Z. S.; Philipenko, O. S.; Aldoshin, S. M.; Shishkin, O. V. *Mendeleev Commun.* **1997**, *7*, 153-154.
[28] Denisova, A. N.; Denisov, E. T.; Metelitsa, D. I. *Russ. Chem. Bull.* **1969**, *8*, 1537-1542.
[29] Chatfield, D. C.; Augsten, A.; D'Cunha, C.; Lewandowska, E.; Wnuk, S. F. *Eur. J. Org. Chem.* **2004**, 313-322.
[30] a) Gornostaev, L. M.; Lyashchenko, T. A.; Arnold, E. V. *Chem. Heter. Compounds* **2014**, *49*, 1827-1830. b) Harmon, R. E.; Myles Phipps, L.; Howell, J. A.; Gupta, S. K. *Tetrahedron* **1969**, *25*, 5807-5813.
[31] a) Blake, A. J.; Grant, C. M.; Parsons, S.; Rawson, J. M.; Winpenny, R. E. P. *J. Chem. Soc., Chem. Commun*. **1994**, 2363-2364. b) Andres, H.; Basler, R.; Blake, A. J.; Cadiou, C.; Chaboussant, G.; Grant, C. M.; Güdel, H.- U.; Murrie, M.; Parsons, S.; Paulsen, C.; Semadini, F.; Villar, V.; Wernsdorfer, W.; Winpenny, R. E. P. *Chem. Eur. J*. **2002**, *8*, 4867-4876.
[32] Bai, Y.; Dang, D.; Duan, C.; Song, Y.; Meng, Q. *Inorg. Chem*. **2005**, *44*, 5972-5974.
[33] a) Grillo, V. A.; Hanson, G. R.; Wang, D.; Hambley, T. W.; Gahan, L. R.; Murray, K. S.; Moubaraki, B.; Hawkins, C. J. *Inorg. Chem.* **1996**, *35*, 3568-3576. b) Boudalis, A. K.; Dahan, F.; Bousseksou, A.; Tuchagues, J.- P.; Perlepes, S. P. *Dalton Trans.* **2003**, 3411-3418.
[34] a) Boudalis, A. K.; Pissas, M.; Raptopoulou, C. P.; Psycharis, V.; Abarca, B.; Ballesteros, R. *Inorg. Chem*. **2008**, *47*, 10674-10681. b) An, G.- Y.; Wang, H.- B.; Cui, A.- L.; Kou, H.- Z. *New J. Chem*. **2014**, *38*, 5037-5042. c) Escuer, A.; Vlahopoulou, G.; Mautner, F. A. *Dalton Trans*. **2011**, *40*, 10109-10116. d) Perivolaris, A.; Stoumpos, C. C.; Karpinska, J.; Ryder, A. G.; Frost, J. M.; Mason, K.; Prescimone, A.; Slawin, A. M. Z.; Kessler, V. G.; Mathieson, J. S.; Cronin, L.; Brechin, E. K.; Papaefstathiou, G. S. *Inorg. Chem. Front*. **2014**, *1*, 487-494. e) Escuer, A.; Esteban, J.; Roubeau, O. *Inorg. Chem*. **2011**, *50*, 8893-8901.
[35] Chilton, N. F.; Anderson, R. P.; Turner, L. D.; Soncini, A.; Murray, K. S. *J. Comput. Chem.* **2013**, *34*, 1164-1175.
[36] Fleischauer, P. D.; Fleischauer, P.; *Chem. Rev.* **1970**, *70*, 199-230.
[37] Bünzli, J.- C. G.; Piguet, C. *Chem. Soc. Rev.* **2005**, *34*, 1048-1077.
[38] a) Lehn, J.- M. *Angew. Chem. Int. Ed.* **1990**, *29*, 1304-1319. b) Binnemans, K. *Chem. Rev.* **2009**, *109*, 4283-4374. c) Chia, Y. Y.; Tay, M. G. *Dalton Trans.* **2014**, *43*, 13159-13168.
[39] Barwiolek, M.; Szlyk, E.; Muziol, T. M.; Lis, T. *Dalton Trans.* **2011**, *40*, 11012-11022.